Vol. 80: 167–180, 2017
https://doi.org/10.3354/ame01847

AQUATIC MICROBIAL ECOLOGY
Aquat Microb Ecol

Published online October 5

Environmental controls on estuarine nitrifying communities along a salinity gradient

Maria Monteiro[1,*], Joana Séneca[1,2], Luís Torgo[2], Daniel F. R. Cleary[3], Newton C. M. Gomes[3], Alyson E. Santoro[4,5], Catarina Magalhães[1]

[1]Novo Edifício do Terminal de Cruzeiros do Porto de Leixões Avenida General Norton de Matos, S/N 4450-208 Matosinhos, Portugal

[2]LIAAD-INESC Porto LA, R. Ceuta 118-6, 4050-190 Porto, Portugal

[3]Department of Biology, CESAM, Universidade de Aveiro, Campus Universitário de Santiago, 3810-193 Aveiro, Portugal

[4]Horn Point Laboratory, University of Maryland Center for Environmental Science, Cambridge, MD 21613, USA

[5]*Present address:* Department of Ecology, Evolution, and Marine Biology, University of California, Santa Barbara, Santa Barbara, CA 93106, USA

ABSTRACT: Estuaries are transitional zones between marine and freshwater environments and are ideal systems to study the influence of environmental gradients on microbial biodiversity and activity. In this study, we investigated the effect of a salinity gradient on the structure of prokaryotic communities from intertidal sediments of the Douro estuary, and on the nitrification process. Four locations were chosen with distinct salinities and characterized for a range of environmental parameters including measurements of potential nitrification rates. The structure of prokaryotic communities and ammonia-oxidizing bacteria and archaea were described and identified using the 16S rRNA gene. Potential nitrification rates ranged from 1.3 to 7.4 µmol cm^{-2} h^{-1}, with the highest rate at mesohaline sites; however, the relative abundance of nitrifying taxa was higher at locations with higher salinity. Ammonia-oxidizing bacteria could not be detected in oligohaline sites, in contrast to ammonia-oxidizing archaea, which showed a ubiquitous distribution. Nitrite-oxidizing bacteria were more abundant than ammonia-oxidizing groups across meso-oligohaline sites, showing increased relative abundance at less saline sites. One operational taxonomic unit closely related to *Nitrospira moscoviensis* showed a positive correlation with potential nitrification rates, suggesting a possible association of *N. moscoviensis* with ammonia-oxidizing organisms in a natural ecosystem. Such results point out the need to re-assess the relative roles of different nitrifying groups in the nitrification process.

KEY WORDS: Estuaries · Salinity · 16S rRNA gene · Nitrification · Nitrifying communities

INTRODUCTION

Estuaries link freshwater and marine systems, creating a highly dynamic environment subjected to extreme fluctuations of salinity, temperature, dissolved oxygen, pH and nutrients (Levin et al. 2001). Such variations influence the structure and composition of microbial communities, which underpin biogeochemical processes in the ecosystem (Lozupone & Knight 2007, Jeffries et al. 2012).

Nitrification has an important role in the equilibrium of estuarine ecosystems (Howarth et al. 2011). It influences primary production and facilitates the removal of nitrogen (N), through denitrification and by the side release of nitrous oxide (N_2O) (Thamdrup 2011, Jung et al. 2014). In other words, nitrification is the linking step between N input and loss back to the atmosphere. Average rates of this process in estuarine sediments can range between 50 and 70 µmol m^{-2} h^{-1} (Henriksen & Kemp 1988); however, such values are

*Corresponding author: mariaroviscomonteiro@gmail.com

likely to change throughout the year, being dependent on local abiotic conditions. That is the case in the Douro estuary (Portugal), where nitrification rates can range seasonally between 2 and 78 nmol NH_4^+ g^{-1} sediment h^{-1} (Magalhães et al. 2009).

Nitrification is usually split into 2 reactions, performed by 2 different groups of microorganisms. The first step — the oxidation of ammonia (NH_3) to nitrite (NO_2^-) — is performed by both ammonia-oxidizing bacteria (AOB) (Koops et al. 2006) and ammonia-oxidizing archaea (AOA) (Könneke et al. 2005). These functional groups are generally diverse and ubiquitous across different ecosystems; however, several studies have reported the existence of niche specialization in both groups, closely related to different abiotic parameters (Erguder et al. 2009, Bernhard & Bollmann 2010, Stahl & de la Torre 2012, Hugoni et al. 2015). A prevalence of AOA over AOB has been observed in waters with lower levels of oxygen (Molina et al. 2010) and NH_4^+ concentrations (Wuchter et al. 2006, Martens-Habbena et al. 2009). A higher transcriptional activity of AOA has also been observed in terrestrial ecosystems with low pH (Gubry-Rangin et al. 2010). Salinity has been pointed out as an important regulator of AOA and AOB distribution and activity (Santoro et al. 2008, Magalhães et al. 2009, Bernhard et al. 2010, Hugoni et al. 2015). This factor not only induces physical transformations in the environment (e.g. NH_4^+ adsorption), altering the availability of N forms (Rysgaard et al. 1999), but also requires physiological adaptation for microorganisms to deal with osmotic stress (Jeffries et al. 2012). The second step of nitrification is performed by a different and polyphyletic group of bacteria known as the nitrite-oxidizing bacteria (NOB). Recently, possible associations between members of the phylum Nitrospirae and ammonia-oxidizing microorganisms (AOM) through a 'reciprocal feeding' mechanism were reported (Koch et al. 2015). It was also discovered that some bacteria belonging to *Nitrospira* genus — comammox bacteria (van Kessel et al. 2015, Daims et al. 2015) — are able to perform the full nitrification process, changing the framework of nitrification and N cycling.

Previous research in the Douro River estuary demonstrated seasonal variation and a positive influence of intermediate salinities on the nitrification (Magalhães et al. 2005a). Additional quantifications of nitrifying communities at the mouth of the estuary showed higher abundances of AOB over AOA, which could indicate AOB as the main contributors for nitrification. Taking advantage of the demarked environmental gradient of Douro estuary, the present study aimed to determine the effect of specific abiotic factors on estuarine prokaryotic communities, with a particular focus on nitrifying communities.

To that purpose, we combined molecular fingerprinting techniques with amplicon sequencing to describe the structure of prokaryotic communities and to identify nitrifying members of the community along the salinity gradient. These analyses were complemented with isotope tracer measurements of nitrification potential to link microbial communities with their biogeochemical signatures.

MATERIALS AND METHODS

Site description and sample collection

The Douro River estuary covers an area of 7.5 km^2 with a watercourse that extends for 21.6 km, flowing into the Atlantic Ocean between the cities of Porto and Gaia, Portugal. The average estuary depth is about 8.2 m; tides are semi-diurnal with an average tidal range of 2.8 m at the mouth and 2.6 m at the head. It is classified as a mesotidal estuary (Vieira & Bordalo 2000). Freshwater discharges average 488 m^3 s^{-1} and the water residence time is between 0.3 and 16.5 d, depending on the season. Under low river flow conditions (summer), the estuary is salinity stratified and considered a salt-wedge estuary (Vieira & Bordalo 2000). The salinity gradient along the estuary can range between 0 and 35 ppt and the temperature between 7°C (winter) and 22°C (summer) (Magalhães et al. 2002). Coastal waters provide an input of dissolved inorganic carbon (DIC) to the estuary, which decreases as salinity decreases. The dissolved organic carbon (DOC) exhibits a non-conservative behaviour along the estuary, mainly due to sewage sources located on the middle and lower estuary (Magalhães et al. 2008). Most N exists as dissolved organic nitrogen (DON) and is mainly supplemented by riverine discharges (Magalhães et al. 2008).

Four locations across the salinity gradient were sampled during low tide in mid-July 2012 (location A: Afurada; location B: Areinho; location C: Avintes; location D: Crestuma). Within each location, intertidal sediments were sampled at 3 sites with a 20 m distance between them, in order to test for any intra-sampling location variability. Intertidal sediments were collected from the top and oxygenated layer (2 cm) using sterilized shovels. The sediment layer was sampled uniformly, stored in sterile plastic bags, homogenized and then transported to the laboratory inside dark, refrigerated ice chests. Three clear acrylic core tubes were used to collect intact sedi-

ment from one site of each sampling location. Sediments were cored to depths of approximately 10 cm, sealed and transported back to the laboratory in dark and cooled conditions. At the laboratory, each core was filled with 250 ml of filtered water collected from each station; however, due to physical and potential chemical destabilization, they were left for 24 h to stabilize under the new laboratory conditions. Adjacent to each sampling location, water samples were taken from the surface of the river, stored in acid-washed flasks and transported back to the laboratory inside dark, refrigerated ice chests. In the laboratory, water samples were filtered using 0.8 µm (GF/F) and 0.45 µm PVDF Whatman pore size filters and analyzed for inorganic forms of nitrogen (NH_4^+, NO_2^-, NO_3^-) using standard colorimetric methods (Magalhães et al. 2002), and total dissolved carbon (TDC), inorganic carbon (IC) and total dissolved nitrogen (TDN). Salinity and temperature were measured *in situ* at the water surface with a multi-parameter probe (Hanna Instruments). Sampling time took between 3 and 4 h. In the laboratory, subsamples of the homogenized sediment were immediately processed for the analysis of inorganic N fluxes, total organic matter (TOM), grain size, total nitrogen (TN) and carbon (TC). The remaining sediment was stored at –20°C for 1 mo before DNA extraction.

Analytical procedures

To assess TOM present in the sediment, samples were dried at 60°C until a constant weight was achieved, incinerated at 500°C for 4 h and reweighed (Magalhães et al. 2002). Sediments were weighed (2 mg) and analyzed using a Flash 2000 elemental analyzer for TC and TN contents (Bahlmann et al. 2010). Grain size was measured by sieving 100 g of previously dried sediment (60°C). Each fraction of sediment was recovered according to its size (<0.063, >0.063, >0.125, >0.25, >0.5, >1 and >2 mm) and reweighed (Magalhães et al. 2002). For water samples, the determination of TDC, IC and TDN was performed using a Shimadzu Instruments TOC-VCSN analyzer coupled to a total nitrogen measuring unit (TNM-1, Shimadzu) according to previously described methods (Magalhães et al. 2008).

Nitrification rates

Potential nitrification rates were measured at each location using ^{15}N isotopic additions to the acrylic cores. At the laboratory, each core was filled with 250 ml of filtered water collected from each sampling location; however, due to physical and possible chemical destabilizations, they were left for 24 h to stabilize to the new laboratory conditions. On the following day, the water was gently poured off and cores were filled again with the same filtered water. Labelled $^{15}N\text{-}NH_4^+$ (20 % of the concentration measured *in situ*) was added to 2 cores while the third was used as a control. The incubation lasted 4 h, and 10 ml of the overlying water was collected in the beginning (time zero) and after 2 and 4 h. The analyses of ^{15}N in the NO_x pool ($^{15}N\text{-}NO_2^-$ and $^{15}N\text{-}NO_3^-$) were performed using the denitrifier method (Sigman et al. 2001). The potential rates were analyzed based on changes in the $^{15}N/^{14}N$ content of the NO_x pool and calculated using Eq. (1) from Dugdale & Goering (1967), but instead of using NO_3^- we used NH_4^+.

Potential nitrification rates were also measured in a 50 ml serum bottle, using the acetylene block technique (Magalhães et al. 2005b), in order to test intra-site variability as well as to compare to the stable isotope tracer experiments. The slurries were set up using 10 ml of sediment from each site, previously mixed and weighed. A total of 20 ml of pre-filtered estuarine water from each location was added to each bottle and incubated for 4 h. At time zero and after 4 h, the overlaying water was collected, centrifuged and filtered.

Inorganic N fluxes

In the cores amended with $^{15}N\text{-}NH_4^+$, concentrations of NH_4^+, NO_3^- and NO_2^- were measured at time zero and after 2 and 4 h of incubation according to previously described methods (Magalhães et al. 2002). The water volume present in the core over the time was taken into account during the calculations. Fluxes of inorganic nutrients were calculated using the slope of the linear relationship of nutrient concentrations in the overlaying water versus incubation time. The slope was then divided by the superficial core area (Magalhães et al. 2002). Positive or negative values of nutrient fluxes corresponded to nutrient effluxes or influxes, respectively.

DNA extraction

Total DNA was extracted from a total of 12 sediment samples (from 3 sites at each location), with duplicates of each sample. A total of 0.5 to 1 g of wet

homogenized sediment was used to extract total DNA using the PowerSoil DNA isolation kit (MoBio Laboratories) according to manufacturer's instructions. The quality of the DNA extracted was verified by running 5 µl of the total DNA in 1.5% agarose gel, stained with SYBR® Safe.

PCR and DGGE analysis

A PCR amplification of the AOA and AOB *amoA* gene (encoding the alpha sub-unit of ammonia monooxigenase) was performed followed by fingerprinting analysis.

For AOA, a single PCR run was performed using the set of primers Cren amoA 23F/Cren amoA 616R (10 µM) (Tourna et al. 2008), under the following conditions: 4 min denaturation at 95°C, 30 thermal cycles of 30 s at 95°C, 30 s at 58°C, and 30 s at 72°C and a final extension step at 72°C for 5 min. For the beta subclass of AOB, a nested PCR was performed using the amoA1F/amoA2R′ (10 µM) primer set (Rotthauwe et al. 1997, Okano et al. 2004) in the first amplification, and the same set of primers in the second amplification with a GC clamp attached to the 5′ end of the forward primer (Table 1). The running conditions were: 5 min at 95°C, 35 thermal cycles of 30 s at 95°C, 30 s at 58°C, and 45 s at 72°C and a final extension step at 72°C for 5 min. The second amplification was done using 1 µl of the previous PCR product and the running conditions only differed in the number of cycles (reduced to 25) and the annealing temperature (increased to 60°C). All PCR reactions were performed in a 25 µl solution using DreamTaq PCR Master Mix (2X) (Life Technologies) and each run included a blank control without template, to ensure there were no contamination issues. PCR products from all the 12 samples were loaded directly into an 8 to 10% polyacrylamide gel with a formamide and urea denaturing gradient of 25 to 45% for AOA and 20 to 58% for AOB, in order to assess the structure of AOA and AOB communities.

DGGE was performed at 70 V for 16 h at 60°C in 1× TAE buffer. Gels were stained using the silver nitrate protocol (Heuer et al. 2001) and fingerprint images were acquired using the Epson Perfection V700 Photo Scanner.

Table 1. Target group and primer sequences used in all PCR DNA amplifications. AOA: ammonia-oxidizing archaea; AOB: ammonia-oxidizing bacteria; NGS: Next Generation Sequence

Target group	Primer	Sequence (5′–3′)
AOA	Cren amoA 23F	ATG GTC TGG CTW AGA CG
	Cren amoA 616R	GCC ATC CAT CTG TAT GTC CA
AOB	amoA1F[a]	GGG GTT TCT ACT GGT GGT
	amoA2R′	CCT CKG SAA AGC CTT CTT C
Bacteria/ Archaea NGS	342F	CTA CGG GGG GCA GCA G
	806R	GGA CTA CCG GGG TAT CT

[a]In the second PCR reaction, the same primer was used, but with a GC clamp attached (GC clamp: 5′-CGC CCG GGG CG CGC CCC GGG CGG GGC GGG GGC ACG GGG GG-3′)

454 sequencing

The V4 hypervariable region of the 16S rRNA gene was amplified in the 12 samples with barcoded fusion primers containing the Roche-454 A and B Titanium sequencing adapters, an 8-base barcode sequence and the primer set 342F/806R (Mori et al. 2014), according to sequencing facility protocols. Two replicate PCR reactions were amplified from 1 µl of each sample, in 20 µl reactions with Advantage Taq (Clontech) using 0.2 µM of each primer, 0.2 mM dNTPs, 5 U of polymerase, 6% DMSO and 2–3 µl of template DNA. The PCR conditions were 95°C for 30 s, followed by 25 cycles of 95°C for 30 s, 55°C for 30 s and 71°C for 15 s and a final elongation step at 72°C for 7 min. Amplicons were quantified by fluorometry with PicoGreen (Invitrogen), pooled at equimolar concentrations and sequenced in the A direction with GS 454 FLX Titanium chemistry, according to manufacturer's instructions (Roche, 454 Life Sciences) at the Biocant sequencing facility (Cantanhede, Portugal). Raw sequencing files were submitted to Sequence Read Archive (SRA) under the accession number SRR5500230.

The barcoded pyrosequencing libraries were analyzed using the QIIME 1.8.0 (Quantitative Insights Into Microbial Ecology) software package (www.qiime.org) (Caporaso et al. 2010a). Fasta and qual files were used as input for the split_libraries.py script. The reverse primer was truncated and sequences with less than 218 nucleotides were discarded, as well as those with a quality score below 50. A denoising step was performed to account for known 454 sequencing errors and to remove singletons (Reeder & Knight 2010). Chimeras were detected and discarded using USEARCH61,

implemented in QIIME (Edgar 2010, Edgar et al. 2011). Operational taxonomic units (OTUs) were defined at a 97% sequence identity cut-off, using the pick_otus.py script with USEARCH61 as the OTU picking method (Edgar 2010). Taxonomy was assigned to representative sequences of each OTU using the default arguments in the assign_taxonomy.py script and GreenGenes database version 13_5 (gg_13_5 OTUs). Finally, the make_otu_table.py script was used to generate a matrix of OTUs. A representative sequence for each OTU was aligned against the reference database using the PyNAST algorithm (Caporaso et al. 2010b) and a phylogenetic tree was constructed from the filtered alignment using the maximum likelihood algorithm implemented in FastTree (Price et al. 2010) and used for further beta diversity inferences.

Nitrifying communities were identified using taxonomic assignments at family (for AOB) and genus levels (for AOA and NOB), with a confidence level higher than 80%.

Statistical analysis

Differences among different locations regarding inorganic N nutrient fluxes and nitrification rates were tested for significance with 1-way ANOVA (Zar 1999) or the Kruskal–Wallis test (K–W) (Kruskal & Wallis 1952), depending on whether assumptions of normality and homogeneity of variances were met, using Statistica version 11 software (Statsoft 2011). Hierarchical clustering analysis (HCA) and a principal component analysis (PCA) using a scaled environmental matrix were computed with Euclidean distance using the vegan package (Oksanen et al. 2013) in R (R Core Team 2013). We tested for differences in the sampling locations according to their salinity using an analysis of similarity (ANOSIM) (Clarke & Warwick 2001).

DGGE gels for *amoA* profiles were analyzed using Bionumerics (version 6.6; Applied Maths) (Smalla et al. 2007). The position and number of bands in the gel were transformed into a binary matrix (presence/absence). The matrix was converted into a dissimilarity matrix using Bray–Curtis distance for HCA analysis in PRIMER 6 (Primer 6 software, PRIMER-E) (Clarke & Warwick 2001). A proxy for richness was calculated by counting the number of bands on the gel for each sample.

Bar plots revealing the relative abundance of bacterial and archaeal phyla were made in Microsoft Excel 2011 using the pyrosequencing 16S rRNA gene dataset. The abundance of all OTUs described in this study was normalized to the number of sequences in each sample and presented as a percentage. Diversity analyses were carried out in QIIME using a dataset rarefied to 3610 sequences per sample. Beta diversity was computed using a weighted UniFrac distance matrix with Jackknife support (Caporaso et al. 2010a) to construct a principal coordinates plot. Heatmaps and Spearman correlation coefficients were generated using Hmisc, corrplot and ggplot2 R packages (Wickham 2009, Wei 2013 and Harrell 2017, respectively).

RESULTS

Environmental characterization of the Douro estuary

Surface water and sediment samples were screened for a variety of environmental parameters (Table 2). Along the estuary, mixing between seawater and freshwater creates several gradients, namely, salinity gradients and chemical gradients such as the decreasing concentration of NH_4^+ and increasing concentration of NO_3^- from the mouth to the head of the estuary (Table 2).

A multivariate statistical analysis (Fig. 1), which included environmental data from the water column and sediments along the estuary, revealed a separation of the samples from marine to freshwater sites along PC1 (explaining 47% of the variance in the data). Samples from location A (Afurada) grouped together, being associated with polyhaline waters (18–30 ppt) enriched in NH_4^+ and depleted in NO_3^-. Sediments from this location contained the highest percentages of silts and clays (fine sediments) (Fig. 1, Table 2). The samples displayed on the left side of the PCA are representative of meso-oligohaline sites (5–18 ppt). Those sites were less influenced by high concentrations of NH_4^+ in the water column but showed increasing concentrations of NO_3^- towards the head of the estuary. PC2 explained 27% of the variance and grouped the samples according to sediment grain size, organic matter, pore water concentrations of NH_4^+ and water C/N ratios (Fig. 1, Table 2).

Nitrification rates and inorganic N fluxes

Nitrification rates were measured in acclimatized cores collected along the salinity gradient from oligo-,

Table 2. Water column and sediment characterization at each of the 4 locations sampled in the Douro estuary. Data are presented as means (±SD) of the 3 sub-sites at each sampling site. The parameters shown from left to right are: latitude and longitude (Lat/Long); total dissolved carbon (TDC); inorganic carbon (IC); total dissolved nitrogen (TDN); C:N ratio; water column concentrations of ammonium (NH_4^+), nitrite (NO_2^-) and nitrate (NO_3^-); salinity; temperature; percentage of organic matter (OM); fraction of carbon (TC) and nitrogen (TN) in the sediment; C:N ratio in the sediment; percentage of fines and gravel in the sediment; and ammonium (NH_4^+), nitrite (NO_2^-) and nitrate (NO_3^-) pore water concentrations

Lat/Long	Water								Sediment						
	TDC (mg l^{-1})	IC (mg l^{-1})	TDN (mg l^{-1})	C:N	NH_4^+ (µM)	NO_2^- (µM)	NO_3^- (µM)	Salinity (ppt)	Temp (°C)	OM %	TC %	TN %	C:N	% Fines	% Gravel	NH_4^+ (µM)	NO_2^- (µM)	NO_3^- (µM)
Afurada (location A)																		
41° 08′ 20″ N	27.74	25.96	1.516	18.3	3.39	0.59	19.77	21.7	18	1.03	24.78	8.54	2.9	4.2	22.17	30.39	1.68	26.94
8° 39′ 14″ W	(–0.1)		(–0.02)		(–1.1)	(–0.03)	(–1.4)			(–0.15)	(–4.5)	(–3.9)	(–1.33)	(–1.01)	(–2.47)	(–6.8)	(–0.16)	(–4.16)
Areinho (location B)																		
41° 08′ 18″ N	24.04	21.98	1.185	20.29	2.55	0.69	42.61	9.3	21.8	0.46	19.32	7.21	2.68	0.11	62.16	44.7	2.52	55.94
8° 35′ 17″ W	(–0.35)		(–0.01)		(–0.2)	(–0.02)	(–0.3)			(–0.01)	(–4.3)	(–1.1)	(–0.28)	(–0.03)	(–5.1)	(–15.6)	(–2.21)	(–20.86)
Avintes (location C)																		
41° 07′ 06″ N	21.25	19.36	1.479	14.37	2.86	0.73	78.23	6.7	22.3	1.08	19.5	7.74	2.52	1.8	43.03	53.37	1.61	110.93
8° 33′ 00″ W	(–0.1)		(–0.04)		(–0.9)	(–0.02)	(–3.9)			(–0.04)	(–1.6)	(–0.4)	(–0.12)	(–0.2)	(–14.03)	(–9.95)	(–1.41)	(–9.38)
Crestuma (location D)																		
41° 04′ 25″ N	22.56	20.34	1.186	19.02	2.51	0.78	61.47	4.9	24.7	0.78	19.4 3	6.6	2.94	1.16	43.08	1.66	0.8	122.07
8° 29′ 27″ W	(–0.35)		(–0.02)		(–0.1)	(–0.02)	(–0.7)			(–0.16)	(–1.7)	(–2.3)	(–1.1)	(–0.3)	(–10.06)	(–2.07)	(–0.15)	(–30.07)

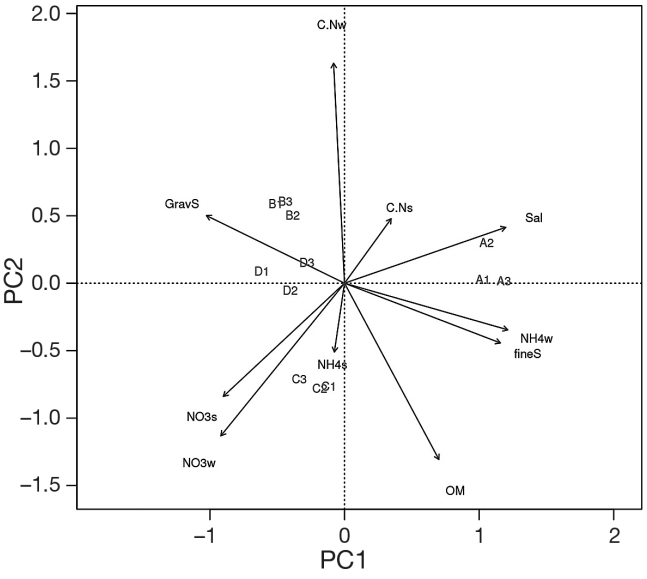

Fig. 1. Principal component analysis (PCA) of all sampling sites based on environmental parameters. Samples and variables (arrows) are displayed for the first 2 axes. Environmental variables represented are: salinity, water column and pore water concentrations of NH_4^+, water column and pore water concentrations of NO_3^-, C/N ratios in the water column and sediments, percentage of organic matter in the sediments (OM), percentage of fine sediments and gravel. Arrows represent the relationship (direction and strength) of the chemical parameters with the samples. PC1 explains 47% and PC2 explains 27% of the variance. See legend to Fig. 6 for abbreviation definitions

meso- and polyhaline sites (Fig. 2A). On average, the rates exhibited a unimodal distribution ranging between 1.3 and 7.4 µmol cm^{-2} h^{-1}, with the highest rate in mesohaline sites (specifically at location C). The results were congruent with measurements of potential nitrification in the slurries using acetylene inhibition techniques, which also showed the highest rates at mid estuarine sites (data not shown). There were significant positive correlations between the measured rates and the pore water concentrations of NH_4^+ (rho = 0.65, $p < 0.05$) and NH_4^+ fluxes (rho = 0.8, $p < 0.05$), as well as with percentages of gravel within the sediments (rho = 0.58, $p < 0.05$).

The sediment efflux of NH_4^+ was higher at mesohaline sites, mainly at location C (Fig. 2B). Net fluxes of NO_2^- were very low, and always on the threshold between effluxes and influxes, which is congruent with the low concentration of NO_2^- in the water column and pore water (Fig. 2C, Table 2). A general influx of NO_3^- into the sediments occurred across all sites, with increasing NO_3^- influx as NO_3^- availability increased (rho = –0.9, $p < 0.05$; Fig. 2D, Table 2), suggesting a higher capacity of these sediments to transform NO_3^-.

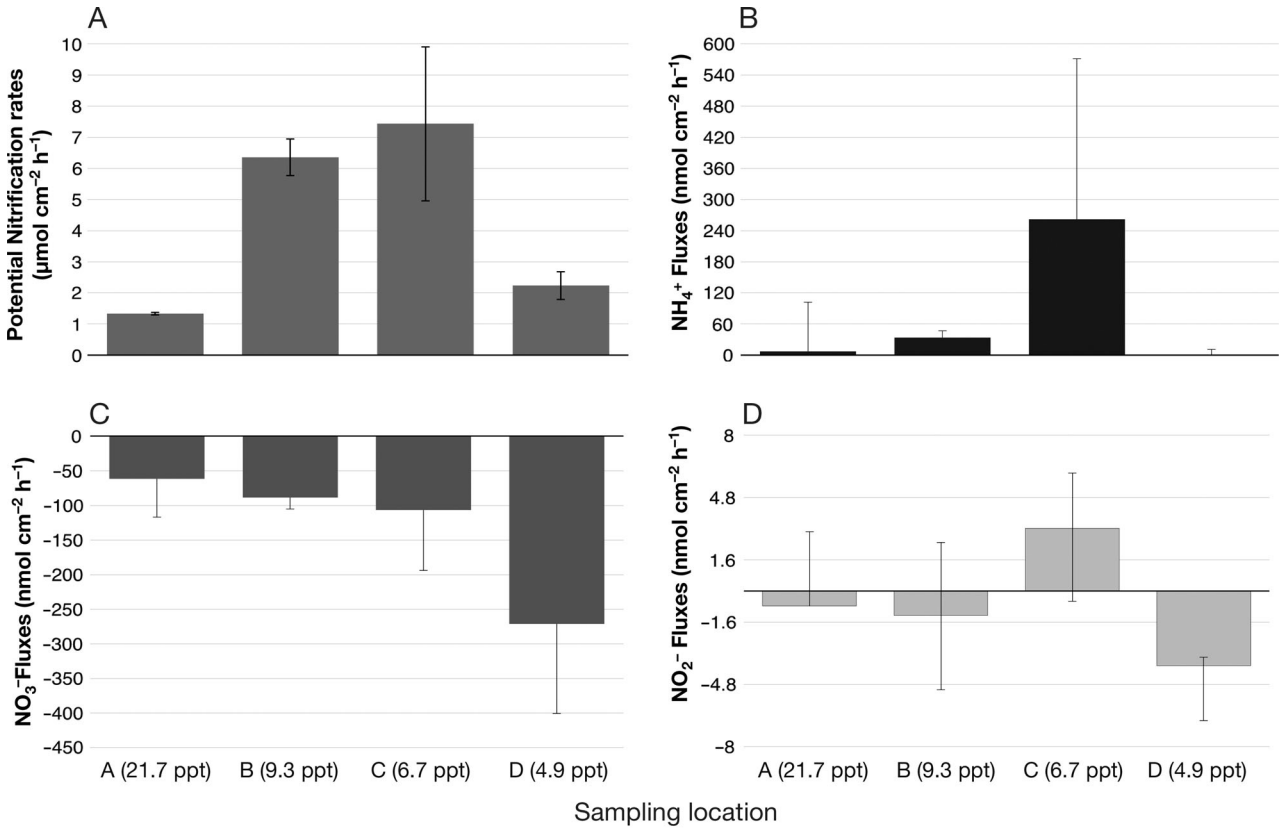

Fig. 2. Means and standard deviations of (A) nitrification potentials using ^{15}N-NH_4^+ additions (n = 2) and (B–D) N inorganic fluxes (B: NH_4^+; C: NO_3^-; D: NO_2^-) (n = 3) across the 4 sampling locations (location A: Afurada; location B: Areinho; location C: Avintes; location D: Crestuma)

Site-related variation in microbial community structure

From a raw sequence input of 113 552 reads, 60 703 16S rRNA gene sequences passed the initial quality-filtering step. Additionally, reads were subjected to a denoising step followed by chimera detection, which resulted in a total of 60 419 sequences ranging from 3931 to 6469 sequences per sample (n = 12). This resulted in 4058 OTUs, including both Archaea (88 reads and 12 OTUs) and Bacteria (59 548 reads and 3684 OTUs).

Prokaryotic communities showed a significant spatial heterogeneity along the estuary (ANOSIM, R = 0.96, p = 0.001, 999 permutations) (Fig. S1 in the Supplement at www.int-res.com/articles/suppl/a080p167_supp.pdf), shifting prominently between locations B and C. Nonetheless, richness and diversity indices calculated from a rarefied dataset did not show any significant variation, except for location B (1-way ANOVA, F = 11.64, p = 0.0027 for richness; 1-way ANOVA, F = 36.45, p < 0.001 for Shannon index).

Certain phyla appeared to be relatively more abundant close to the mouth of the estuary (e.g. Proteobacteria, Bacteroidetes, SR1 phyla) whereas other phyla seemed to have a preference for less saline sites (e.g. Acidobacteria, Nitrospirae, Chloroflexi and Planctomycetes) (Fig. S2 in the Supplement). The shifts in the structure of the microbial community are also shown at the family level (using families whose relative abundance was higher than 1%), reinforcing the spatial microbial heterogeneity along the estuary (Fig. 3). The Flavobacteriaceae, Phormidiaceae, Marinicellaceae, Piscirickettsiaceae and Rhodobacteraceae families had higher relative abundances at higher salinities and low NO_3^- concentrations, contrasting with Xanthomonadaceae, Hyphomicrobiaceae, Comamonadaceae and C111 families, which were better represented at less saline sites (Fig. 3)

In regard to the Archaea, most of OTUs were affiliated with the phylum Thaumarchaeota. Their relative abundance was low (average of 0.1% across the estuary), possibly due to PCR primer coverage, but they showed a ubiquitous distribution throughout the estuary.

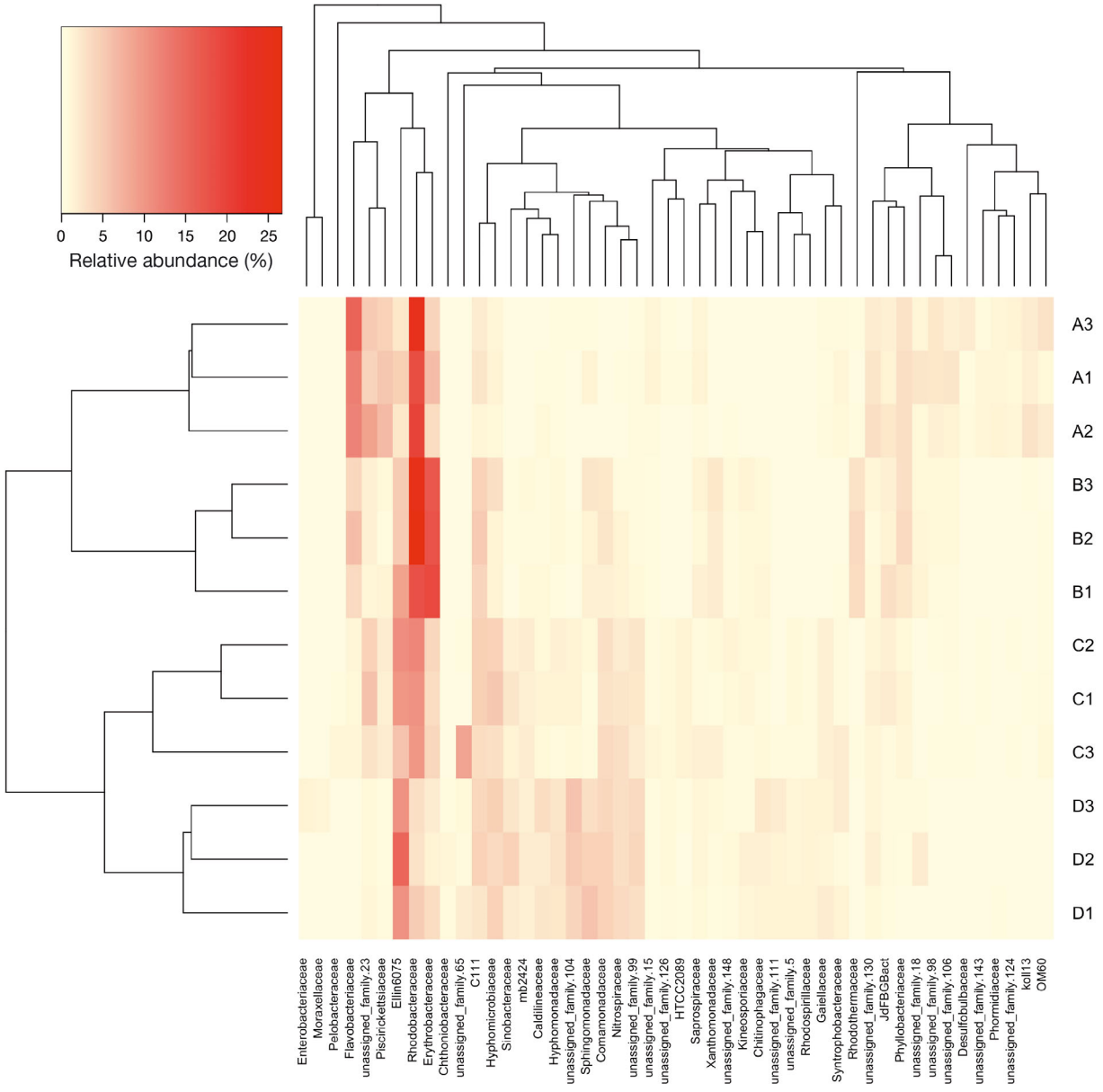

Fig. 3. Heatmap of the relative abundance (%) of prokaryotic communities at family level arranged by hierarchical clustering (average linking) and based on community similarity along the salinity gradient. The dataset represents a subset of the families found with a total relative abundance greater than 1% using a non-rarefied matrix. The scale represents the relative abundance (%) of each family at each sampling site. Upper dendrogram depicts clustering of family by co-occurrence (average linkage clustering). Left dendrogram represents a hierarchical clustering (average linkage clustering) using Bray–Curtis dissimilarity distance on the full family dataset. Codes A1, A2 and A3 refer to location A (Afurada); B1, B2, B3 to location B (Areinho); C1, C2, C3 to location C (Avintes); and D1, D2, D3 to location D (Crestuma)

Nitrifying community structure along the estuarine gradient

The relative abundance of nitrifying organisms comprised 0.5 and 2.4% of all sequences along the estuary. With respect to AOM, both AOA (mostly represented by OTUs affiliated with the genus *Nitrosopumilus*, 6 OTUs) and AOB (only represented by OTUs affiliated with the family Nitrosomonadaceae, 5 OTUs) showed higher relative abundances at the highest saline sites (0.20 and 0.25%, respectively). However, while AOB relative abundance declined along the salinity gradient (not detected in the upper part of the estuary), AOA relative abundance ranged

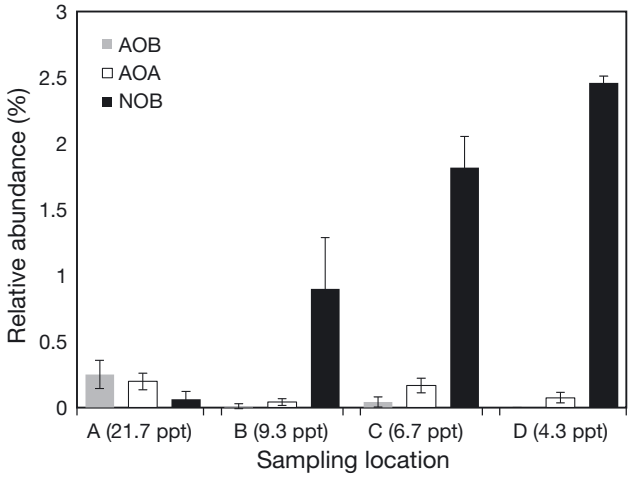

Fig. 4. Relative abundance (%) of nitrifying organisms along the 4 estuarine sampling locations. AOB: ammonia-oxidizing bacteria; AOA: ammonia-oxidizing archaea; NOB: nitrite-oxidizing bacteria

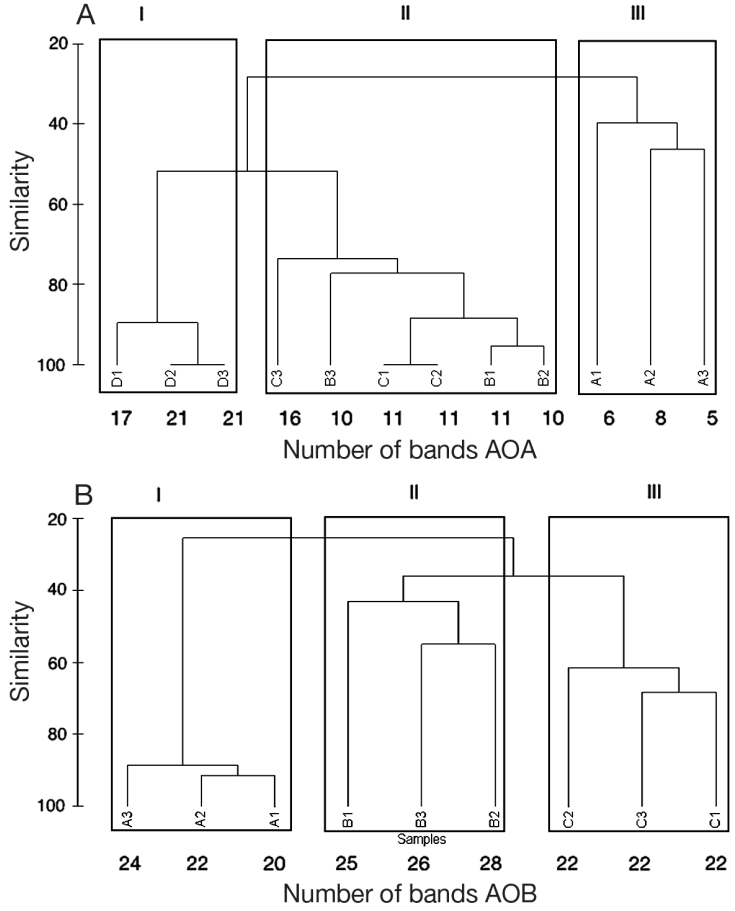

Fig. 5. Hierarchical cluster analysis (group average linking using Bray–Curtis similarity) of (A) archaeal and (B) bacterial *amoA* genes from DGGE profiles across the estuarine salinity gradient. I: polyhaline sites; II: mesohaline sites; III: oligohaline sites. A presence/absence matrix was used as an input file. For AOB, the absence of location D was due to the unsuccessful amplification of the gene for that location. The significance of the cluster was tested with ANOSIM ($p < 0.05$)

between 0.04 and 0.16% along the rest of the estuary (Fig. 4). With respect to NOB, the *Nitrospira* genus was present in all sampling locations (from 0.06 to 2.5%) and especially in the upper part of the estuary, where its relative abundance was 32 times higher than that of AOM (Fig. 4).

AmoA gene profile along the estuarine gradient

Community structure of AOM was additionally assessed by DGGE based on *amoA* gene gel profiles. The number of bands on AOA gels increased as salinity increased (rho = −0.96, $p < 0.05$) (Fig. 5A), and *amoA* profiles clustered according to salinity (ANOSIM, $R = 0.684$, $p < 0.01$). Pairwise comparisons showed R-values equal to 1 for comparison between locations A (polyhaline site) and D (oligohaline site), and non-significant R-values were obtained for comparisons between locations B and C ($R = 0.37$, $p = 0.1$), revealing that AOA communities from mesohaline sites displayed a very similar structure (Fig. 5A). In contrast, the number of bands on AOB gels did not decline with decreasing salinity, but the *amoA* gene could not be detected in the less saline site, consistent with the 16S rRNA gene results. The genotypic profiles of *amoA* differed significantly among locations ($R = 1$, $p < 0.05$), and even between the 2 mesohaline sites (Fig. 5B).

Effect of the estuarine abiotic gradient on nitrifying community composition

The correlation heatmaps performed for OTUs affiliated with nitrifying taxa highlighted the presence of different groups with specific abiotic factors. Specific nitrifying communities were positively and significantly ($p < 0.05$) related to salinity and higher NH_4^+, TN and TC water column concentrations (Fig. 6B, Table 2). This included AOB OTU_2 and OTU_5 (0.02 and 0.21%, respectively), affiliated with the family Nitrosomonadaceae, and AOA OTU_5, affiliated with the genus *Nitrosopumilus* (0.17%) (Fig. 6A). The presence of these organisms was restricted to location A (Fig. 6A). With respect to NOB, no OTUs significantly related to high salinity locations were found (Fig. 6B).

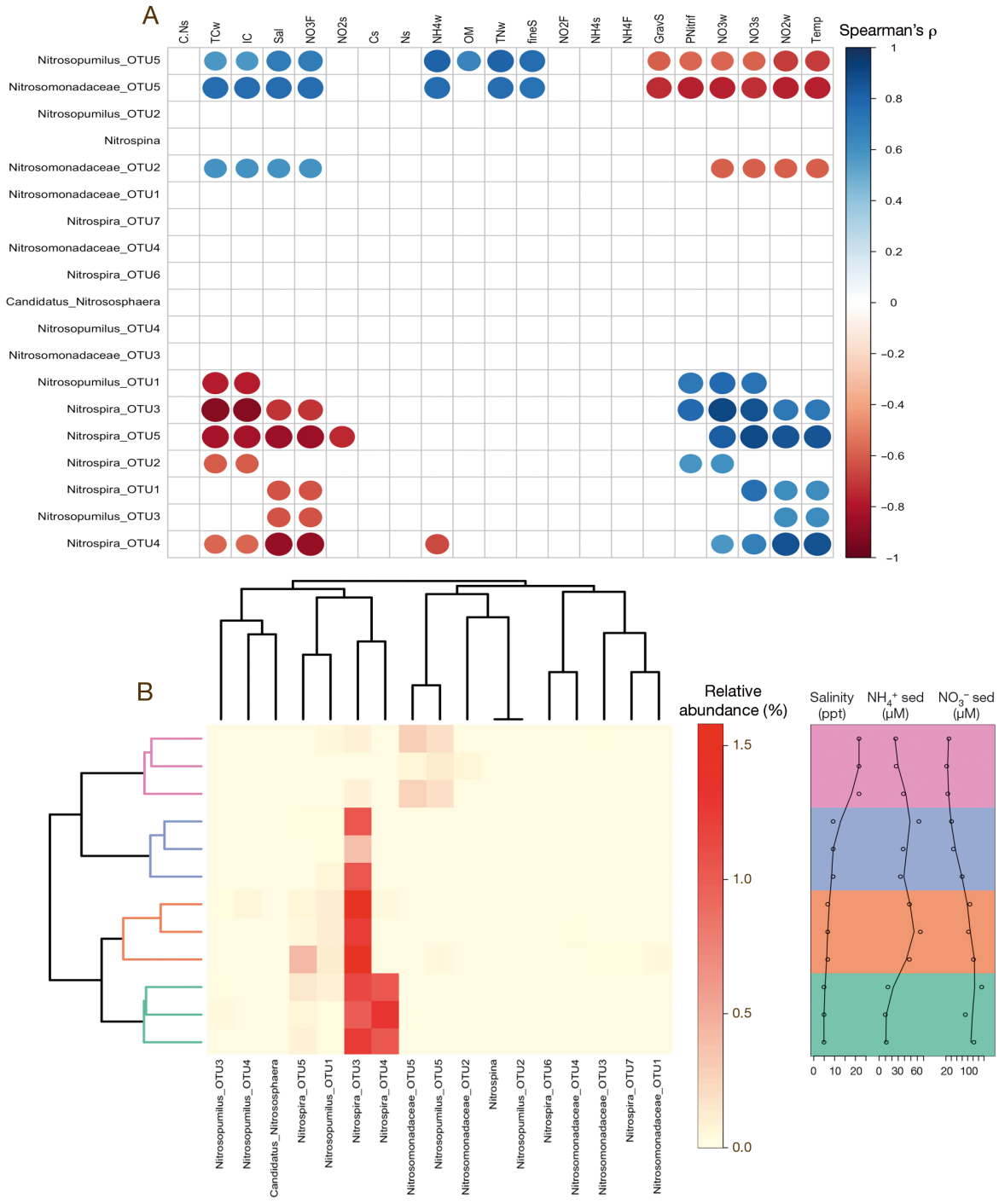

Fig. 6. (A) Heatmap showing significant Spearman correlations (circles) between OTUs affiliated with nitrifying organisms and the main environmental variables measured at each site. Positive correlations are displayed in blue and negative correlations in red. Color intensity and the size of each circle are proportional to the correlation coefficient. C.Ns: C:N ratios in the sediment; TCw: total carbon in the water column; IC: inorganic carbon present in the water column; Sal: salinity (ppt); NO3F: nitrate fluxes; NO2s: pore water nitrite concentration; Cs: total carbon present in the sediment; Ns: total nitrogen present in the sediment; NH4w: water column ammonia concentration (µM); OM: percentage of organic matter in the sediment; TNw: total nitrogen present in the water column; fineS: percentage of fines in the sediment; NO2F: nitrite fluxes; NH4s: pore water ammonia concentration (µM); NH4F: ammonia fluxes; GravS: percentage of gravel in the sediment; PNitrif: potential nitrification rates; NO3w: water column nitrate concentration (µM); NO3s: pore water nitrate concentration (µM); NO2w: water column nitrite concentration (µM); Temp: temperature (°C). (B) Heatmap representations of the relative abundance (%) of OTUs related to the nitrifying community along the estuarine transect. Along the left axis is a dendrogram of sampling sites (average linking) based on community similarity (pink: location A; blue: location B; orange: location C; green: location D). Upper dendrogram depicts clustering of OTUs by co-occurrence (average linking). Right-hand panel shows the environmental variables salinity and NH_4^+ and NO_3^- concentrations in the sediment

In meso-oligohaline sites characterized by NO_3^- enriched waters, the majority of the ammonia-oxidizing OTUs were affiliated with the genus *Nitrosopumilus* (OTU_1 and OTU_3; 0.08 and 0.01%, respectively) (Fig. 6B). The archaeal OTU_1 was particularly abundant at location C (0.11%) and was positively correlated with nitrification rates (rho = 0.71, p = 0.009; Fig. 6B).

Regarding NOB, the relative abundance of the genus *Nitrospira* increased 0.8% from location A to B and kept increasing up to the oligohaline site, where members of this genus represented 2.5% of the prokaryotic community (Fig. 5). Significant correlations were observed between phylotypes of this genus and specific abiotic parameters from meso-oligohaline sites (Fig. 6B). The most abundant OTU was *Nitrospira* OTU_3 (average of 0.87%), which was predominant at all locations across the estuary except at the most saline site (Fig. 6A). Due to its high abundance, we blasted this sequence against the NCBI database and the closest cultivable representative was *Nitrospira moscoviensis* (E value = 0; identity 99%; accession number AF155153.1). Other NOB groups such as *Nitrospira* OTU_2 and OTU_5 were also abundant at locations with mesohaline conditions (average of 0.1% at locations B and C), contrasting with groups formed by *Nitrospira* OTU_1 and OTU_4, which only occurred in the upper part of the estuary (locations C and D) (Fig. 6A). Those had a significant negative relationship with NO_3^- and NO_2^- concentrations in the water (Fig. 6B).

DISCUSSION

Bacteria and Archaea from intertidal sediments play important roles in the dynamics of estuaries; however, physical and chemical gradients can exert a great influence on the structure and function of these communities (Herlemann et al. 2011, Fortunato et al. 2012, Zheng et al. 2014).

In this study, we demonstrated that prokaryotic communities from the Douro estuary are not constant and change throughout the estuary. Differences in the chemical and physical properties of the water and sediment, possibly related to the location of the sampling sites, could be the reason for the structural shifts in microbial communities (Fortunato et al. 2012). Salinity has been reported to be a factor with a strong influence in the estuarine microbiome (Lozupone & Knight 2007). Our analyses showed that different families were positively influenced by salinity, such as Flavobacteriaceae (Bacteroidetes phylum), Phormidiaceae (Cyanobacteria phylum), Marinicellaceae, Piscirickettsiaceae and Rhodobacteraceae (Proteobacteria phyla), while families such as Xanthomonadaceae, Hyphomicrobiaceae, Comamonadaceae and C111 had lower relative abundances in saline sites. Alterations in community structure entail changes in biogeochemical processes, as most of these processes are controlled by microbial activity. For example, a previous study showed that taxonomic shifts reflected an increased abundance of genes encoding for halotolerance and photosynthesis, which likely influence nutrient cycles of the entire ecosystem (Jeffries et al. 2012).

Nitrification has a global impact on the availability of nitrogen forms in the ecosystem. However, the rates of this process are seasonal and dependent on environmental conditions (Magalhães et al. 2009). Along the Douro estuary, the highest potential rates were recorded at mesohaline sites, confirming previous results from controlled experiments (Magalhães et al. 2005a) and estuarine isolates (Jones & Hood 1980, Macfarlane & Herbert 1984). Nonetheless, the values reported here are higher than the ones recorded previously (Magalhães et al. 2009). A possible explanation could be the application of 2 different methods — the acetylene block method and the use of stable N isotopes — which prevent an absolute comparison between the values obtained. Despite the lack of significant correlations with salinity, the rates measured were significantly influenced by the percentage of gravel in the sediments and NH_4^+ concentrations, which has been suggested to stimulate the activity of estuarine nitrifying communities (Bernhard et al. 2007).

Along the Douro estuary, AOA and AOB 16S rRNA gene relative abundance ranged between 0.04–0.19% and 0–0.25%, respectively, which, although similar to the values described in other studies (Hollibaugh et al. 2011, Li et al. 2015), may still be affected by incomplete coverage of the PCR primers used in this study. It is also possible that unknown nitrifying taxa were present in the samples; however, since they are not classified in genetic databases, their detection is not possible through 16S rRNA amplicon sequencing. The capability of ammonia oxidation has been recently found in new microorganisms, whose *amoA* genes would not be amplified with the standard primers used to identify nitrifying organisms (Bernhard et al. 2010, Daims et al. 2015).

The relative abundance of AOM was higher at the highest salinity site, with a dominance of AOB over AOA. This is in agreement with previous quantifications of the bacterial *amoA* performed at the same

site (Magalhães et al. 2009) and in other estuaries (Mosier & Francis 2008, Santoro et al. 2008); however, it contrasts with results from another study (Hugoni et al. 2015). Surprisingly, a marked reduction of AOB occurred as salinity decreased, culminating with a non-detection of AOB at the least saline site, which was also reinforced by the non-detection of bacterial *amoA* in those same samples by PCR. These results suggest the absence or a negligible occurrence of AOB in the upper part of the estuary during the sampling season, which is interesting because AOB are frequently found in freshwater systems (Koops et al. 2006, Hugoni et al. 2015, Li et al. 2015). In contrast, AOA communities showed a more even distribution, outnumbering AOB in meso- and oligohaline locations, suggesting greater adaptability and a broader distribution over the estuarine gradient.

Results from 16S rRNA gene and *amoA* DGGE profiles showed the existence of different ammonia-oxidizing populations across the estuary, which reinforces the impact of abiotic conditions, in particular salinity, in shaping the distribution and structure of these populations (Bernhard et al. 2007, Hugoni et al. 2015, Zhao et al. 2015). Two OTUs appeared to be highy related to higher salinities, namely, OTU_5, assigned to the family Nitrosomonadaceae, and OTU_5, assigned to the genus *Nitrosopumilus*. This was consistent with AOA and AOB *amoA* DGGE profiles, which showed significant dissimilarities between samples from the mouth of the estuary and those from the rest of this ecosystem, highlighting a possible presence of autochthonous marine phylotypes (Smith et al. 2014) more adapted to salinity fluctuations (Bernhard et al. 2007). In mesohaline locations, a marked shift occurred in ammonia-oxidizing community composition. Not only was *Nitrosopumilus* OTU_1 predominant across less saline locations, but *amoA* profiles were also very similar at these locations. Concerning AOB populations, despite the existence of different ecotypes, their relative abundance was very low. Nevertheless, the results from both methodologies show that the structure of the community changed along the estuarine salinity gradient.

NOB complete the process of nitrification through the oxidation of NO_2^- to NO_3^- (Abeliovich 2006). The members of this group observed in our study were affiliated with the genus *Nitrospira* and their relative abundance increased from 0.06 to 2.45% throughout the estuary, being mainly predominant at meso- and oligohaline sites, and 32 times more abundant than AOM at the less saline site. This is an interesting observation due to the recent discovery of candidate species of *Nitrospira* capable of performing the full nitrification pathway (comammox) (Daims et al. 2015, van Kessel et al. 2015). Similar to AOM, NOB seemed to be strongly influenced by salinity, as shown by the sudden increase in their abundance as salinity dropped and by the presence of distinctive phylotypes along the salinity gradient. While *Nitrospira* OTU_4 was restricted to the oligohaline site, *Nitrospira* OTU_3 was abundant across both meso- and oligohaline sites. Moreover, this OTU (affiliated with *N. moscoviensis* according to our BLAST results) was positively correlated with potential nitrification rates, which could indicate a possible association with AOA (Koch et al. 2015). Therefore, it was suggested that the metabolic flexibility of *N. moscoviensis* could allow it to be more abundant and successful in the colonization of different niches, compared with AOM (Koch et al. 2015). We believe the higher relative abundance of these species and the positive correlations with the potential nitrification rates could reflect this prediction, showing the ecological advantage of *Nitrospira* species in the environment and their role in the nitrification process.

CONCLUSIONS

In this study, we observed differences in the structure of the prokaryotic community along the Douro estuary. These differences could be driven by the salinity gradient of the estuary, which also influenced nitrifying functional groups. An interesting discovery was the contrast between AOM (higher relative abundance at more saline sites) and NOB (higher relative abundance at less saline sites, where AOB were not detected). Our results and the recent discoveries relating to NOB, in particular the predominance of OTUs affiliated with the genus *Nitrospira* and its positive correlation with potential nitrification rates, highlight the need to re-assess the relative role of each group of nitrifying organisms in the environment.

Acknowledgements. We thank Ana Paula Mucha, Sandra Ramos, Paula Salgado and Ana Pires for their assistance with fieldwork, data analysis and technical support. This work was supported by the Portuguese Science and Technology Foundation through a research grant to C. Magalhães [AMOX/PTDC/MAR/112723/2009]. This research was partially supported by the Structured Program of R&D&I CORAL – NORTE-01-0145-FEDER-000036 and MarInfo – NORTE-01-0145-FEDER-000031, funded by the NORTE2020 through the European Regional Development Fund (ERDF).

LITERATURE CITED

Abeliovich A (2006) The nitrite oxidizing bacteria. The prokaryotes. Springer, New York, NY

Bahlmann E, Bernasconi SM, Bouillon S, Houtekamer M, and others (2010) Performance evaluation of nitrogen isotope ratio determination in marine and lacustrine sediments: an inter-laboratory comparison. Org Geochem 41:3–12

Bernhard AE, Bollmann A (2010) Estuarine nitrifiers: new players, patterns and processes. Estuar Coast Shelf Sci 88:1–11

Bernhard AE, Tucker J, Giblin AE, Stahl DA (2007) Functionally distinct communities of ammonia oxidizing bacteria along an estuarine salinity gradient. Environ Microbiol 9:1439–1447

Bernhard AE, Landry ZC, Blevins A, José R, Giblin AE, Stahl DA (2010) Abundance of ammonia-oxidizing archaea and bacteria along an estuarine salinity gradient in relation to potential nitrification rates. Appl Environ Microbiol 76:1285–1289

Caporaso JG, Kuczynski J, Stombaugh J, Bittinger K and others (2010a) QIIME allows analysis of high-throughput community sequencing data. Nat Methods 7: 335–336

Caporaso JG, Bittinger K, Bushman FD, DeSantis TZ, Andersen GL, Knight R (2010b) PyNAST: a flexible tool for aligning sequences to a template alignment. Bioinformatics 26:266–267

Clarke KR, Warwick RM (2001) Change in marine communities: an approach to statistical analysis and interpretation, 2nd edn. PRIMER-E, Plymouth

Daims H, Lebedeva EV, Pjevac P, Han P and others (2015) Complete nitrification by Nitrospira bacteria. Nature 528:504–509

Dugdale R, Goering J (1967) Uptake of new and regenerated forms of nitrogen in primary productivity. Limnol Oceanogr 12:196–206

Edgar RC (2010) Search and clustering orders of magnitude faster than BLAST. Bioinformatics 26:2460–2461

Edgar RC, Haas BJ, Clemente JC, Quince C, Knight R (2011) UCHIME improves sensitivity and speed of chimera detection. Bioinformatics 27:2194–2200

Erguder TH, Boon N, Wittebolle L, Marzorati M, Verstraete W (2009) Environmental factors shaping the ecological niches of ammonia-oxidizing archaea. FEMS Microbiol Rev 33:855–869

Fortunato CS, Herfort L, Zuber P, Baptista AM, Crump BC (2012) Spatial variability overwhelms seasonal patterns in bacterioplankton communities across a river to ocean gradient. ISME J 6:554–563

Gubry-Rangin C, Nicol GW, Prosser JI (2010) Archaea rather than bacteria control nitrification in two agricultural acidic soils. FEMS Microbiol 74:566–574

Harrell FE Jr (2017) Hmisc: Harrell miscellaneous. R package version 4.0-3. https://CRAN.R-project.org/package=Hmisc

Henriksen K, Kemp WM (1988) Nitrification in estuarine and coastal marine sediments. In: Blackburn TH, Sørensen J (eds) Nitrogen cycling in coastal marine environments, Vol 33. John Wiley & Sons, Chichester, p 207–249

Herlemann DP, Labrenz M, Jürgens K, Bertilsson S, Waniek JJ, Andersson AF (2011) Transitions in bacterial communities along the 2000 km salinity gradient of the Baltic Sea. ISME J 5:1571–1579

Heuer H, Wieland G, Schönfeld J, Schönwälder A, Gomes N, Smalla K (2001) Bacterial community profiling using DGGE or TGGE analysis. Environ Mol Microbiol Protoc Appl 9:177–190

Hollibaugh JT, Gifford S, Sharma S, Bano N, Moran MA (2011) Metatranscriptomic analysis of ammonia-oxidizing organisms in an estuarine bacterioplankton assemblage. ISME J 5:866–878

Howarth R, Chan F, Conley DJ, Garnier J, Doney SC, Marino R, Billen G (2011) Coupled biogeochemical cycles: eutrophication and hypoxia in temperate estuaries and coastal marine ecosystems. Front Ecol Environ 9:18–26

Hugoni M, Agogué H, Taib N, Domaizon I and others (2015) Temporal dynamics of active prokaryotic nitrifiers and archaeal communities from river to sea. Microb Ecol 70: 473–483

Jeffries T, Seymour J, Newton K, Smith R, Seuront L, Mitchell J (2012) Increases in the abundance of microbial genes encoding halotolerance and photosynthesis along a sediment salinity gradient. Biogeosciences 9:815–825

Jones RD, Hood MA (1980) Effects of temperature, pH, salinity, and inorganic nitrogen on the rate of ammonium oxidation by nitrifiers isolated from wetland environments. Microb Ecol 6:339–347

Jung MY, Well R, Min D, Giesemann A and others (2014) Isotopic signatures of N2O produced by ammonia-oxidizing archaea from soils. ISME J 8:1115–1125

Koch H, Lücker S, Albertsen M, Kitzinger K and others (2015) Expanded metabolic versatility of ubiquitous nitrite-oxidizing bacteria from the genus *Nitrospira*. Proc Natl Acad Sci USA 112:11371–11376

Könneke M, Bernhard AE, José R, Walker CB, Waterbury JB, Stahl DA (2005) Isolation of an autotrophic ammonia-oxidizing marine archaeon. Nature 437:543–546

Koops HP, Purkhold U, Pommerening-Röser A, Timmermann G, Wagner M (2006) The lithoautotrophic ammonia-oxidizing bacteria. In: Dworkin M, Falkow S, Rosenberg E, Schleifer KH, Stackebrandt E (eds) The prokaryotes. Springer, New York, NY, p 778–811

Kruskal WH, Wallis WA (1952) Use of ranks in one-criterion variance analysis. J Am Stat Assoc 47:583–621

Levin LA, Boesch DF, Covich A, Dahm C and others (2001) The function of marine critical transition zones and the importance of sediment biodiversity. Ecosystems 4: 430–451

Li J, Nedwell DB, Beddow J, Dumbrell AJ, McKew BA, Thorpe EL, Whitby C (2015) amoA gene abundances and nitrification potential rates suggest that benthic ammonia-oxidizing bacteria and not archaea dominate N cycling in the Colne Estuary, United Kingdom. Appl Environ Microbiol 81:159–165

Lozupone CA, Knight R (2007) Global patterns in bacterial diversity. Proc Natl Acad Sci USA 104:11436–11440

Macfarlane G, Herbert R (1984) Effect of oxygen tension, salinity, temperature and organic matter concentration on the growth and nitrifying activity of an estuarine strain of *Nitrosomonas*. FEMS Microbiol Lett 23:107–111

Magalhães CM, Bordalo AA, Wiebe WJ (2002) Temporal and spatial patterns of intertidal sediment-water nutrient and oxygen fluxes in the Douro River estuary, Portugal. Mar Ecol Prog Ser 233:55–71

Magalhães CM, Wiebe WJ, Joye SB, Bordalo AA (2005a) Inorganic nitrogen dynamics in intertidal rocky biofilms and sediments of the Douro River estuary (Portugal). Estuaries 28:592–607

Magalhães CM, Joye SB, Moreira RM, Wiebe WJ, Bordalo AA (2005b) Effect of salinity and inorganic nitrogen concentrations on nitrification and denitrification rates in intertidal sediments and rocky biofilms of the Douro River estuary, Portugal. Water Res 39:1783–1794

Magalhães C, Teixeira C, Teixeira R, Machado A, Azevedo I, Bordalo A (2008) Dissolved organic carbon and nitrogen dynamics in the Douro River estuary, Portugal. Cienc Mar 34:271–282

Magalhães CM, Machado A, Bordalo AA (2009) Temporal variability in the abundance of ammonia-oxidizing bacteria vs. archaea in sandy sediments of the Douro River estuary, Portugal. Aquat Microb Ecol 56:13–23

Martens-Habbena W, Berube PM, Urakawa H, José R, Stahl DA (2009) Ammonia oxidation kinetics determine niche separation of nitrifying Archaea and Bacteria. Nature 461:976–979

Molina V, Belmar L, Ulloa O (2010) High diversity of ammonia oxidizing archaea in permanent and seasonal oxygen deficient waters of the eastern South Pacific. Environ Microbiol 12:2450–2465

Mori H, Maruyama F, Kato H, Toyoda A and others (2014) Design and experimental application of a novel non-degenerate universal primer set that amplifies prokaryotic 16S rRNA genes with a low possibility to amplify eukaryotic rRNA genes. DNA Res 21:217–227

Mosier AC, Francis CA (2008) Relative abundance and diversity of ammonia oxidizing archaea and bacteria in the San Francisco Bay estuary. Environ Microbiol 10: 3002–3016

Okano Y, Hristova KR, Leutenegger CM, Jackson LE and others (2004) Application of real-time PCR to study effects of ammonium on population size of ammonia-oxidizing bacteria in soil. Appl Environ Microbiol 70: 1008–1016

Oksanen J, Blanchet FG, Kindt R, Legendre P and others (2013) Package 'vegan'. Community ecology package, version 2. R package version 2.4-3, https://CRAN.R-project.org/package=vegan

Reeder J, Knight R (2010) Rapid denoising of pyrosequencing amplicon data: exploiting the rank-abundance distribution. Nat Methods 7:668–669

Rotthauwe JH, Witzel KP, Liesack W (1997) The ammonia monooxygenase structural gene amoA as a functional marker: molecular fine-scale analysis of natural ammonia-oxidizing populations. Appl Environ Microbiol 63: 4704–4712

Rysgaard S, Thastum P, Dalsgaard T, Christensen PB, Sloth NP (1999) Effects of salinity on NH_4^+ adsorption capacity, nitrification, and denitrification in Danish estuarine sediments. Estuaries 22:21–30

Santoro AE, Francis CA, De Sieyes NR, Boehm AB (2008) Shifts in the relative abundance of ammonia oxidizing bacteria and archaea across physicochemical gradients in a subterranean estuary. Environ Microb 10:1068–1079

Sigman DM, Casciotti KL, Andreani M, Barford C, Galanter M, Böhlke JK (2001) A bacterial method for the nitrogen isotopic analysis of nitrate in seawater and freshwater. Anal Chem 73:4145–4153

Smalla K, Oros-Sichler M, Milling A, Heuer H and others (2007) Bacterial diversity of soils assessed by DGGE, T-RFLP and SSCP fingerprints of PCR-amplified 16S rRNA gene fragments: do the different methods provide similar results? J Microbiol Methods 69:470–479

Smith JM, Casciotti KL, Chavez FP, Francis CA (2014) Differential contributions of archaeal ammonia oxidizer ecotypes to nitrification in coastal surface waters. ISME J 8:1704–1714

Stahl DA, de la Torre JR (2012) Physiology and diversity of ammonia-oxidizing archaea. Annu Rev Microbiol 66: 83–101

Thamdrup B (2011) New pathways and processes in the global nitrogen cycle. Annu Rev Ecol Evol Syst 43:407–428

Tourna M, Freitag TE, Nicol GW, Prosser JI (2008) Growth, activity and temperature responses of ammonia oxidizing archaea and bacteria in soil microcosms. Environ Microbiol 10:1357–1364

van Kessel MA, Speth DR, Albertsen M, Nielsen PH and others (2015) Complete nitrification by a single microorganism. Nature 528:555–559

Vieira ME, Bordalo AA (2000) The Douro estuary (Portugal): a mesotidal salt wedge. Oceanol Acta 23:585–594

Wei T (2013) Corrplot: visualization of a correlation matrix. https://CRAN.R-project.org/package=corrplot

Wickham H (2009) ggplot2: elegant graphics for data analysis. Springer Verlag, New York, NY, http://ggplot2.org

Wuchter C, Abbas B, Coolen MJ, Herfort L and others (2006) Archaeal nitrification in the ocean. Proc Natl Acad Sci USA 103:12317–12322

Zar J (1999) Biostatistical analysis. Prentice Hall, Upper Saddle River, NJ

Zhao J, Wang B, Jia Z (2015) Phylogenetically distinct phylotypes modulate nitrification in a paddy soil. Appl Environ Microbiol 81:3218–3227

Zheng B, Wang L, Liu L (2014) Bacterial community structure and its regulating factors in the intertidal sediment along the Liaodong Bay of Bohai Sea, China. Microbiol Res 169:585–592

Editorial responsibility: Tom Battin, Vienna, Austria

Submitted: November 15, 2016; Accepted: June 23, 2017
Proofs received from author(s): August 31, 2017